

Titanium Hydrazido and Imido Complexes: Synthesis, Structure, Reactivity, and Relevance to Alkyne Hydroamination

Yahong Li, Yanhui Shi, and Aaron L. Odom*

Contribution from the Department of Chemistry, Michigan State University,
East Lansing, Michigan 48824

Received September 3, 2003; E-mail: odom@cem.msu.edu.

Abstract: Treatment of $\text{Ti}(\text{NMe}_2)_2(\text{dpma})$ (**1**) with aniline results in the protonation of the dimethylamido ligands, which are retained as dimethylamines, and generation of a titanium imido complex $\text{Ti}(\text{NPh})(\text{NHMe}_2)_2(\text{dpma})$ (**2**) in 94% yield. The monomeric imido **2** is converted to the reactive dimeric μ -imido $[\text{Ti}(\text{NPh})(\text{dpma})]_2$ (**3**) on removal of the labile dimethylamine donors. The dimer **3** is converted to monomeric terminal imido complexes in the presence of added donors, e.g., 4,4'-di-*tert*-butyl-2,2'-bipyridine ($\text{Bu}^t\text{-bpy}$) and DME. Compounds **1–3** exhibit the same rate constant for 1-phenylpropyne hydroamination by aniline and are all kinetically competent to be involved in the catalytic cycle. Attempts to use **1** as a catalyst for hydroaminations involving 1,1-dimethylhydrazine resulted in only a few turnovers under the best conditions. Consequently, the chemistry of **1** with hydrazines to generate hydrazido complexes was scrutinized for comparison with the imido species. Through these studies, titanium hydrazido complexes including $\text{Ti}(\eta^2\text{-NHNHC}_5\text{H}_{10})_2(\text{dpma})$ (**5**), $\text{Ti}(\eta^2\text{-NHNMe}_2)_2(\text{dpma})$ (**6**), and $[\text{Ti}(\mu\text{-}\eta^1, \eta^2\text{-NNMe}_2)(\text{dpma})]_2$ (**7**) were characterized. In addition, a terminal hydrazido(2-) complex was available by addition of $\text{Bu}^t\text{-bpy}$ to **1** prior to 1,1-dimethylhydrazine addition, which provided $\text{Ti}(\eta^1\text{-NNMe}_2)(\text{Bu}^t\text{-bpy})(\text{dpma})$ (**8**). Compound **8** was structurally characterized and compared to $\text{Ti}(\text{NPh})(\text{Bu}^t\text{-bpy})(\text{dpma})$ (**4b**), an imido derivative with the same ancillary ligand set. Compound **8** has a nucleophilic β -nitrogen consistent with a hydrazido(2-) formulation, as determined by reaction with MeI to form the ammonium imido complex $[\text{Ti}(\text{NNMe}_3)(\text{Bu}^t\text{-bpy})(\text{dpma})]\text{I}$ (**9**). Analogous pyridinium imido complexes $[\text{Ti}(\text{N-1-pyridinium})(\text{Bu}^t\text{-bpy})(\text{dpma})]^+$ (**10**) are available by addition of 1-aminopyridinium iodide to **1**. From the investigations, some conclusions regarding the activity of titanium pyrrolyl complexes in hydroamination were drawn. The lack of conversion of the bis(μ -hydrazido(2-)) **7** to monomeric species in the presence of donor ligands is put forth as one explanation for the poor hydrazine hydroamination activity of **1**. This problem was combated in the synthesis of $\text{Ti}(\text{NMe}_2)_2(\text{dap})_2$, which is an active catalyst for hydrazine hydroamination of alkynes.

Introduction

In large part, investigation of hydrazido complexes has been driven by studies of dinitrogen reduction to ammonia.¹ Likely intermediates in that process include N–N-bonded species (azo, hydrazido, and hydrazine complexes), which can impart interesting electronic and reactivity properties to metal complexes.² Due to the composition of the nitrogenase active site, which can incorporate both early and late transition metals (e.g., vanadium, molybdenum, and iron), studies on ligands bearing N–N bonds have extended across the periodic table.

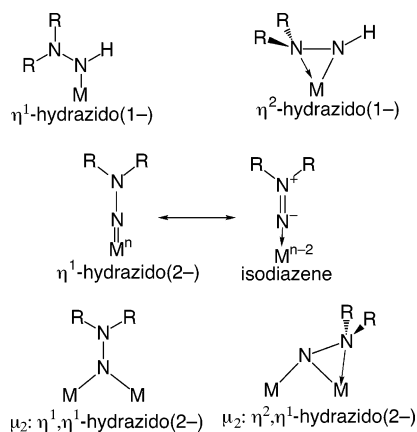
Hydrazido ligands may have several bonding modes to transition metal centers.³ First, the coordination is classified by the formal charge on the hydrazido ligand, which with the 1,1-dialkylhydrazido ligands used here is limited to -1 or -2 . Second, the metal may be bound to either one (η^1) or both (η^2)

nitrogens of the hydrazido. Third, the ligand may be terminal to a single metal or bridging to two (μ_2) or more metal centers. A few of the various bonding modes available and all of the

(1) For reviews on nitrogenase activity, see: (a) Malinak, S. M.; Coucouvanis, D. *Prog. Inorg. Chem.* **2001**, *49*, 599–662. (b) Dilworth, M. J.; Glenn, A. P. *Biology and Biochemistry of Nitrogen Fixation*; Elsevier: Amsterdam, 1991. (c) Stiefel, E. I.; George, G. N. Ferredoxins, Hydrogenases, and Nitrogenases: Metal-Sulfide Proteins. In *Bioinorganic Chemistry*; Bertini, I., Gray, H. B., Lippard, S. J., Valentine, J. S., Eds.; University Science Books: Mill Valley, CA, 1994.

(2) Selected recent examples of dinitrogen reactivity, see: (a) Yandulov, D. V.; Schrock, R. R. *J. Am. Chem. Soc.* **2002**, *124*, 6252–6253. (b) Laplaza, C. E.; Johnson, M. J. A.; Peters, J.; Odom, A. L.; Kim, E.; Cummins, C. C.; George, G. N.; Pickering, I. J. *J. Am. Chem. Soc.* **1996**, *118*, 8623. (c) Smith, J. M.; Lachicotte, R. J.; Pittard, K. A.; Cundari, T. R.; Lukat-Rodgers, G.; Rodgers, K. R.; Holland, P. L. *J. Am. Chem. Soc.* **2001**, *123*, 9222–3. (d) Fryzuk, M. D.; Johnson, S. A.; Patrick, B. O.; Albinati, A.; Mason, S. A.; Koetzle, T. F. *J. Am. Chem. Soc.* **2001**, *123*, 3960–3973. (e) Odom, A. L.; Arnold, P. L.; Cummins, C. C. *J. Am. Chem. Soc.* **1998**, *120*, 5836–5837. (f) Caselli, A.; Solari, E.; Scopelliti, R.; Floriani, C.; Re, N.; Rizzoli, C.; Chiesi-Villa, A. *J. Am. Chem. Soc.* **2000**, *122*, 3652–3670. (g) Hori, K.; Mori, M. *J. Am. Chem. Soc.* **1998**, *120*, 7651–7652. (h) Solari, E.; Da Silva, C.; Iacono, B.; Hesschenbrouck, J.; Rizzoli, C.; Scopelliti, R.; Floriani, C. *Angew. Chem., Int. Ed.* **2001**, *40*, 3907–3909. (i) Hidai, M. *Chem. Rev.* **1995**, *95*, 1115–1133. (j) Horn, K. H.; Lehnert, N.; Tuzcek, F. *Inorg. Chem.* **2003**, *42*, 1076–1086. (k) Yandulov, D. V.; Schrock, R. R. *Science* **2003**, *301*, 76–78. (l) Pool, J. A.; Lobkovsky, E.; Chirik, P. J. *J. Am. Chem. Soc.* **2003**, *125*, 2241–2251. (m) Pool, J. A.; Lobkovsky, E.; Chirik, P. J. *Organometallics* **2003**, *22*, 2797–2805. (n) Baumann, R.; Stumpf, R.; Davis, W. M.; Liang, L. C.; Schrock, R. R. *J. Am. Chem. Soc.* **1999**, *121*, 7822–7836.

(3) For a more complete discussion of hydrazido bonding and reviews, see: (a) Nugent, W. A.; Haymore, B. L. *Coord. Chem. Rev.* **1980**, *31*, 123–175. (b) Nugent, W. A.; Mayer, J. M. *Metal–Ligand Multiple Bonds*; John Wiley & Sons: New York, 1988. (c) Sutton, D. *Chem. Rev.* **1993**, *93*, 995–1022.

Chart 1. Some Relevant Bonding Modes for 1,1-Dialkylhydrazido Ligands and Associated Nomenclature

forms relevant to this work are shown in Chart 1. The usual nomenclature for the structures, as used throughout the remainder of this paper, is shown below each structure.

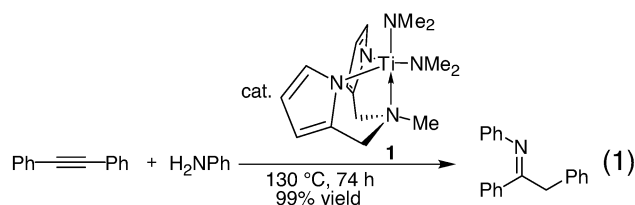
In addition, terminal η^1 -hydrazido(2-) complexes may have several resonance forms owing to the potential participation of the lone pair on the β -nitrogen. Very strong donation from the β -nitrogen lone pair and weak π -donation from the metal center results in a dominant isodiazeno resonance form, which is found for many transition metal complexes.⁴ However, in circumstances where the metal complex would be strongly reducing in the $n - 2$ formal oxidation state, e.g. titanium(II), the hydrazido resonance form should dominate (vide infra).⁵ Consequently, a circumstance reminiscent of the electronic structures of transition metal carbenes⁶ is found where the carbene may be described as a Schrock-type, triplet carbene with the metal in a high formal oxidation state, which is similar to the terminal hydrazido(2-) resonance form. The alternative description is a Fischer-type singlet carbene with the metal in a low formal oxidation state, which is analogous to the isodiazeno resonance form with a strongly donating β -nitrogen lone pair. Substantial reactivity differences are expected as one proceeds through the spectrum of possible electronic structures for the multiple-bond substituent.

While many hydrazido complexes have been generated and characterized for the transition metals, the known hydrazido complexes of titanium⁷ remain relatively limited. For example, reports on η^1 -hydrazido(2-) complexes of titanium are restricted to three systems. The earliest report belongs to Wiberg and co-workers, who provided evidence for the titanocene complex $(\text{Me}_3\text{Si})_2\text{N}=\text{N}=\text{TiCp}_2$.⁸ Utilizing the Schiff-base ligand TMTAA, Mountford and co-workers described the synthesis and reactivity of $\text{Ph}_2\text{N}=\text{N}=\text{Ti}(\text{TMTAA})$.⁹ Most recently, Woo and Thorman

described the synthesis and reactivity of titanium porphyrin complexes of the type $\text{R}_2\text{N}=\text{N}=\text{Ti}(\text{TPP})$.^{10,11} In related chemistry, Leigh and co-workers published a series of papers¹² on titanium monocyclopentadienyl complexes bearing hydrazine-derived ligands including bridging hydrazido(2-) containing $[\text{Ti}(\mu\text{-NNPh}_2)\text{CICp}]_2$, which contains a $\mu^2: \eta^2, \eta^1$ -hydrazido(2-) and a $\mu^2: \eta^1, \eta^1$ -hydrazido(2-) ligand.

More common are reports of hydrazido(1-) complexes of titanium.¹³ Fully characterized complexes in this genre usually have incorporated cyclopentadienyl, tris(pyrazolyl)borate, or halide supporting ligands.¹⁴

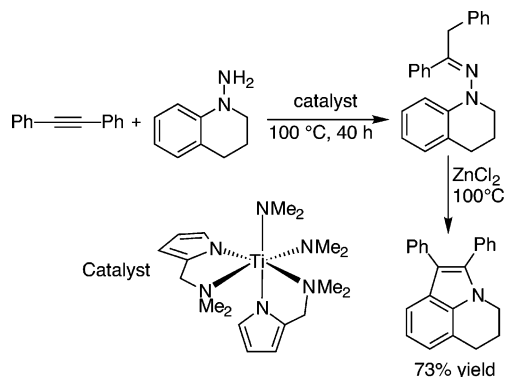
Using pyrrolyl-based ancillary ligands, we have been exploring the catalytic chemistry of titanium complexes. Specifically, $\text{Ti}(\text{NMe}_2)_2(\text{dpma})$ (**1**), where dpma is *N,N*-di(pyrrolyl- α -methyl)-*N*-methylamine¹⁵ (dpma), is an effective hydroamination catalyst for alkynes with primary amines¹⁶ (eq 1) and related transformations such as iminoamination.¹⁷



In one attempt to broaden the scope of hydroamination catalysis, a 1,1-disubstituted hydrazine was used in place of

(4) For seminal examples of isodiazeno complexes, see: (a) Mahy, J.-P.; Battioni, P.; Mansuy, D.; Fisher, J.; Weiss, R.; Mispelter, J.; Morgenstern-Badarau, I.; Gans, P. *J. Am. Chem. Soc.* **1984**, *106*, 1699–1706. (b) Danopoulos, A. A.; Wilkinson, G.; Williams, D. J. *J. Chem. Soc., Dalton Trans.* **1994**, 907–915 and references therein. (5) For some in depth discussions of hydrazido electronic structure, see: (a) DuBois, D. L.; Hoffmann, R. *Nouv. J. Chim.* **1977**, *1*, 479–492. (b) Kahlal, S.; Saillard, J.-Y.; Hamon, J.-R.; Manzur, C.; Carrillo, D. *J. Chem. Soc., Dalton Trans.* **1998**, 1229–1240. (c) Kahlal, S.; Saillard, J.-Y.; Hamon, J.-R.; Manzur, C.; Carrillo, D. *New J. Chem.* **2001**, *25*, 231–242. (6) Gallop, M. A.; Roper, W. R. *Adv. Organometallic Chem.* **1986**, *25*, 121–198. (7) For an example of a zirconium hydrazido(2-) complex, see: Walsh, P. J.; Carney, M. J.; Bergman, R. G. *J. Am. Chem. Soc.* **1991**, *113*, 6343–6345. (8) Wiberg, N.; Häring, H.-W.; Huttner, G.; Friedrich, P. *Chem. Ber.* **1978**, *111*, 2708–2715.

(9) Blake, A. J.; McInnes, J. M.; Mountford, P.; Nikonov, G. I.; Swallow, D.; Watkin, D. J. *J. Chem. Soc., Dalton Trans.* **1999**, 379–391. (10) Thorman, J. L.; Woo, L. K. *Inorg. Chem.* **2000**, *39*, 1301–1304. (11) For related diazoalkane complexes of titanium in a low formal oxidation state, see: (a) Kaplan, A. W.; Polse, J. L.; Ball, G. E.; Andersen, R. A.; Bergman, R. G. *J. Am. Chem. Soc.* **1998**, *120*, 11649–11662. (b) Polse, J. L.; Kaplan, A. W.; Andersen, R. A.; Bergman, R. G. *J. Am. Chem. Soc.* **1998**, *120*, 6316–6328. (c) Gambarotta, S.; Floriani, C.; Chiesi-Villa, A.; Guastini, C. *J. Am. Chem. Soc.* **1983**, *105*, 7295–7301. (d) Gambarotta, S.; Floriani, C.; Chiesi-Villa, A.; Guastini, C. *J. Chem. Soc., Chem. Commun.* **1982**, 1015–1017. For an example of a zirconium diazoalkane complex, see: Arvanitis, G. M.; Schwartz, J.; Van Engen, D. *Organometallics* **1986**, *5*, 2157–2159. (12) (a) Hughes, D. L.; Latham, I. A.; Leigh, G. J. *J. Chem. Soc., Dalton Trans.* **1986**, 393–398. (b) Latham, I. A.; Leigh, G. J. *J. Chem. Soc., Dalton Trans.* **1986**, 399–401. (13) (a) Latham, I. A.; Leigh, G. J.; Huttner, G.; Jibril, I. *J. Chem. Soc., Dalton Trans.* **1986**, 385–391. (b) Hughes, D. L.; Jimenez-Tenorio, M.; Leigh, G. J.; Walker, D. G. *J. Chem. Soc., Dalton Trans.* **1989**, 2389–2395. (c) Hughes, D. L.; Leigh, G. J.; Walker, D. G. *J. Chem. Soc., Dalton Trans.* **1989**, 1413–1416. (d) Kim, S.-J.; Jung, I. N.; Yoo, B. R.; Cho, S.; Ko, J.; Kim, S. H.; Kang, S. O. *Organometallics* **2001**, *20*, 1501–1503. (e) Rep, M.; Kaagman, J.-W. F.; Elsevier, C. J.; Sedmera, P.; Hiller, J.; Thewalt, U.; Horacek, M.; Mach, K. *J. Organometallic Chem.* **2000**, *597*, 146–156. (f) Park, J. T.; Yoon, S. C.; Bae, B.-J.; Seo, W. S.; Suh, I.-H.; Han, T. K.; Park, J. R. *Organometallics* **2000**, *19*, 1269–1276. (g) Rep, M.; Kaagman, J.-W.; Elsevier, C. J.; Sedmera, P.; Hiller, J.; Thewalt, U.; Horacek, M.; Mach, K. *J. Organometallic Chem.* **2000**, *597*, 146–156. (h) Yoon, S. C.; Bae, B.-J.; Suh, I.-H.; Park, J. T. *Organometallics* **1999**, *18*, 2049–2051. (i) Zippel, T.; Arndt, P.; Ohff, A.; Spannenberg, A.; Kempe, R.; Rosenthal, U. *Organometallics* **1998**, *17*, 4429–4437. (j) Ohff, A.; Zippel, T.; Arndt, P.; Spannenberg, A.; Kempe, R.; Rosenthal, U. *Organometallics* **1998**, *17*, 1649–1651. (k) Hill, J. E.; Fanwick, P. E.; Rothwell, I. P. *Inorg. Chem.* **1991**, *30*, 1143–4. (l) Kim, S.-J.; Jung, I. N.; Yoo, B. R.; Cho, S.; Ko, J.; Kim, S. H.; Kang, S. O. *Organometallics* **2001**, *20*, 1501–3. (m) Park, J. T.; Yoon, S. C.; Bae, B.-J.; Seo, W. S.; Suh, I.-H.; Han, T. K.; Park, J. R. *Organometallics* **2000**, *19*, 1269–1276. (n) Hemmer, R.; Thewalt, U.; Hughes, D. L.; Leigh, G. J.; Walker, D. G. *J. Organometallic Chem.* **1987**, *323*, C29–C32. (o) Kiremire, E. M. R.; Leigh, G. J.; Dilworth, J. R.; Henderson, R. A. *Inorg. Chim. Acta* **1984**, *83*, L83–L85. (p) Dilworth, J. R.; Latham, I. A.; Leigh, G. J.; Huttner, G.; Jibril, I. *J. Chem. Soc., Chem. Commun.* **1983**, 1368–1370. (q) Reetz, M. T.; Steinbach, R.; Kesseler, K. *Angew. Chem., Int. Engl.* **1982**, *21*, 864. (r) Goetze, B.; Knizek, J.; Nöth, H.; Schnick, W. *Eur. J. Inorg. Chem.* **2000**, 1849–1854. (s) Lehn, J.-S. M.; Hoffman, D. M. *Inorg. Chim. Acta* **2003**, *345*, 327–332. (t) Schepfer, J. T.; McKarns, P. J.; Lewkebandara, T. S.; Winter, C. H. *Mater. Sci. Semicond. Process.* **1999**, *2*, 149–157. (14) For a related titanium *sym*-hydrazido(2-), see: (a) Fochi, G.; Floriani, C.; Bart, J. C.; Giunchi, G. *J. Chem. Soc., Dalton Trans.* **1983**, 1515–1521. Also see ref 13c and 13d.

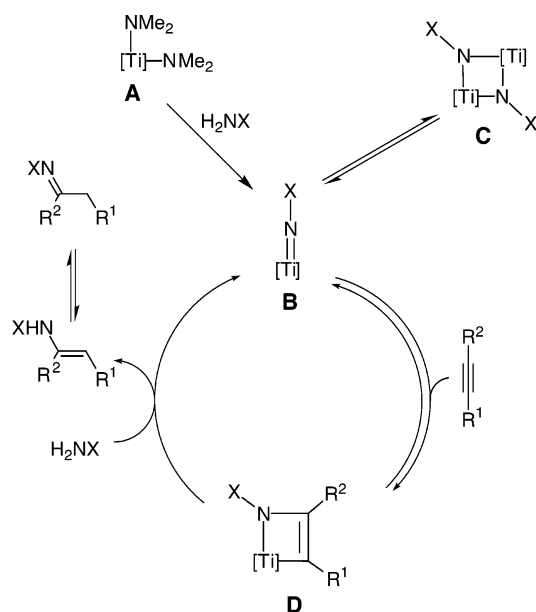
Scheme 1. Example of a Successful Hydroamination Reaction with Hydrazines

primary amine for alkyne hydroamination. While titanium dpma complexes were quite effective with primary amines, they provided only a few turnovers with hydrazines as substrates under the same conditions. Isolating the cause of the poor catalytic activity of **1** led to the present study on the synthesis, structure, and reaction chemistry of titanium hydrazido complexes.

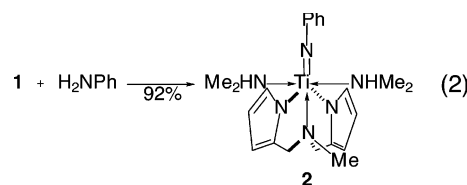
With the aid of the studies discussed here, we were able to develop simple, effective catalysts for the desired transformation.¹⁸ With the improved titanium catalysts, hydrazones are available directly from alkynes, and indoles can be prepared in a one-pot procedure. An example of hydrazine hydroamination with one of the catalysts developed is shown in Scheme 1, which used bis(dimethylaminomethylpyrrolyl)bis(dimethylamido)-titanium(IV), $\text{Ti}(\text{NMe}_2)_2(\text{dap})_2$. By analogy with the mechanism for primary amine hydroamination (Figure 1),^{19,20} the titanium system needs to access a titanium–nitrogen double-bond complex (**B**), which can occur through reaction of the bis(amido) precatalyst (**A**) with the H_2NX species. The Ti–N multiple bond can undergo [2 + 2] cycloaddition with alkynes to form a metalloazacyclobutene intermediate and the new C–N bond. Consequently, we sought to prepare and characterize terminal hydrazido(2-) complexes of titanium with pyrrolyl-based ligands.

Results and Discussion

Synthesis and Reactivity of Titanium dpma Imido Complexes. To better understand the reactivity of titanium hydrazido

**Figure 1.** Simplified mechanistic scheme for alkyne hydroamination (X = aryl, alkyl, or NR_2).

complexes, we first synthesized imido titanium species bearing the dpma ancillary ligand. Titanium imido complexes²¹ are well-known and better understood than their hydrazido analogues.²² Consequently, the imido compounds provide an important framework for understanding hydrazido chemistry.



One of the key reactions that led to the discovery of the hydroamination reactivity of the titanium dpma system is the reaction of $\text{Ti}(\text{NMe}_2)_2(\text{dpma})$ (**1**) with aniline, which is shown in eq 2. Treatment of the bis(dimethylamido) complex with 1 equiv of aniline generates a pseudo-octahedral terminal imido $\text{Ti}(\text{NPh})(\text{dpma})(\text{NHMe}_2)_2$ (**2**) in 92% recrystallized yield. The

- (15) Li, Y.; Turnas, A.; Ciszewski, J. T.; Odom, A. L. *Inorg. Chem.* **2002**, *41*, 6298.
 (16) Cao, C.; Ciszewski, J. T.; Odom, A. L. *Organometallics* **2001**, *20*, 5011–5013. Cao, C.; Ciszewski, J. T.; Odom, A. L. *Organometallics* **2002**, *21*, 5148.
 (17) Cao, C.; Shi, Y.; Odom, A. L. *J. Am. Chem. Soc.* **2003**, *125*, 2880–2881.
 (18) Cao, C.; Shi, Y.; Odom, A. L. *Org. Lett.* **2002**, *4*, 2853–2856.
 (19) We are assuming a mechanism comparable to that of Group-4 catalysis using primary amines. For references on amine hydroamination, see: (a) Pohlki, F.; Doye, S. *Angew. Chem., Int. Ed. Engl.* **2001**, *40*, 2305–2308. (b) Johnson, J. S.; Bergman, R. G. *J. Am. Chem. Soc.* **2001**, *123*, 2923–2924. (c) Siebeneicher, H.; Doye, S. *J. Prakt. Chem. Chem. Ztg.* **2000**, *341*, 102–106. (d) Haak, E.; Bytschkov, I.; Doye, S. *Angew. Chem., Int. Ed. Engl.* **1999**, *38*, 3389–3391. (e) Bytschkov, I.; Doye, S. *Eur. J. Org. Chem.* **2001**, 4411–4418. (f) Shi, Y.; Ciszewski, J. T.; Odom, A. L. *Organometallics* **2001**, *20*, 3967–3969. (g) Cao, C.; Ciszewski, J. T.; Odom, A. L. *Organometallics* **2001**, *20*, 5011–5013. (h) Straub, B. F.; Bergman, R. G. *Angew. Chem., Int. Ed. Engl.* **2001**, *40*, 4632–4635. (i) Sweeney, Z. K.; Salsman, J. L.; Anderson, R. A.; Bergman, R. G. *Angew. Chem., Int. Ed. Engl.* **2000**, *39*, 2339–2343. (j) Polse, J. L.; Anderson, R. A.; Bergman, R. G. *J. Am. Chem. Soc.* **1998**, *120*, 13405–13414. (k) Baranger, A. M.; Walsh, P. J.; Bergman, R. G. *J. Am. Chem. Soc.* **1993**, *115*, 2753–2763. (l) Walsh, P. J.; Baranger, A. M.; Bergman, R. G. *J. Am. Chem. Soc.* **1992**, *114*, 1708–1719.
 (20) For an excellent review of hydroamination chemistry, see: (a) Muller, T. E.; Beller, M. *Chem. Rev.* **1998**, *98*, 675–703. For a unique perspective on the field titanium hydroamination, see: (b) Bytschkov, I.; Doye, S. *Eur. J. Org. Chem.* **2003**, 935–946. (c) Pohlki, F.; Doye, S. *Chem. Soc. Rev.* **2003**, *32*, 104–114.

- (21) Review of transition metal imido complexes, see: Wigley, D. E. *Prog. Inorg. Chem.* **1994**, *42*, 239–482.
 (22) For some examples of titanium imido complexes, see: (a) Hill, J. E.; Profflet, R. D.; Fanwick, P. E.; Rothwell, I. P. *Angew. Chem., Int. Ed.* **1990**, *29*, 664–665. (b) Buchateau, R.; Williams, A. J.; Gambarotta, S.; Chiang, M. Y. *Inorg. Chem.* **1991**, *30*, 4863–4866. (c) Bai, Y.; Notemeyer, M.; Roesky, H. W. *Z. Naturforsch.* **1991**, *46B*, 1357–1363. (d) Winter, C. H.; Sheridan, P. H.; Lewkebandara, T. S.; Heeg, M. J.; Proscia, J. W. *J. Am. Chem. Soc.* **1992**, *114*, 1095–1097. (e) Zambrano, C. H.; Profflet, R. D.; Hill, J. E.; Fanwick, P. E.; Rothwell, I. P. *Polyhedron* **1993**, *12*, 689–708. (f) Dunn, S. C.; Batsanov, A. S.; Mountford, P. *Chem. Commun.* **1994**, 2007–8. (g) Mountford, P.; Swallow, D. *Chem. Commun.* **1995**, 2357–9. (g) Collier, P. E.; Dunn, S. C.; Mountford, P.; Shishkin, O. V.; Swallow, D. *J. Chem. Soc., Dalton Trans.* **1995**, 3743–5. (h) Berreau, L. M.; Young, V. G., Jr.; Woo, L. K. *Inorg. Chem.* **1995**, *34*, 527–529. (i) Bennett, J. L.; Wocznanski, P. T. *J. Am. Chem. Soc.* **1997**, *119*, 10696–10719. (j) Putzer, M. A.; Neumüller, B.; Dehnicke, K. *Z. Anorg. Allg. Chem.* **1998**, *624*, 57–64. (k) Blake, A. J.; Dunn, S. C.; Green, J. C.; Jones, N. M.; Moody, A. G.; Mountford, P. *Chem. Commun.* **1998**, 1235–6. (l) Hagadorn, J. R.; Arnold, J. *Organometallics* **1998**, *17*, 1355–1368. (m) Steinhuebel, D. P.; Lippard, S. J. *Inorg. Chem.* **1999**, *38*, 6225–6233. (n) Blake, A. J.; Collier, P. E.; Gade, L. H.; Mountford, P.; Lloyd, J.; Pugh, S. M.; Schubart, M.; Skinner, M. E. G.; Trösch, D. J. M. *Inorg. Chem.* **2001**, *40*, 870–7. (o) Dooxsee, I. K. M.; Farahi, J. B.; Hope, H. *J. Am. Chem. Soc.* **1991**, *113*, 8889–8898. (p) Trösch, D. J. M.; Collier, P. E.; Bashall, A.; Gade, L. H.; McPartlin, M.; Mountford, P.; Radojevic, S. *Organometallics* **2001**, *20*, 3308–3313. Thorn, D. L.; Nugent, W. A.; Harlow, R. L. *J. Am. Chem. Soc.* **1981**, *103*, 357–363.

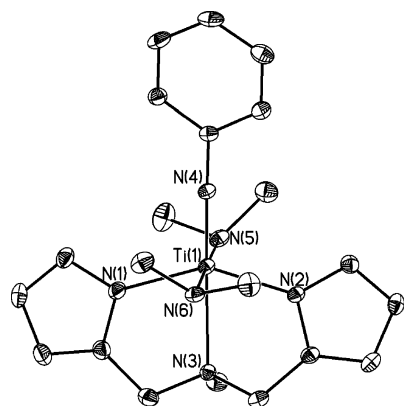


Figure 2. ORTEP representation for the structure of $\text{Ti}(\text{NPh})(\text{NHMe}_2)_2(\text{dpma})$ (**2**) from X-ray diffraction. Ellipsoids are at the 25% probability level.

Table 1. Selected Bond Distances (Å) and Angles (deg) from the X-ray Diffraction Study on $\text{Ti}(\text{NPh})(\text{dpma})(\text{NHMe}_2)_2$ (**2**)

| | | | |
|---------------|----------|--------------|----------|
| Ti–N(1) | 2.071(3) | Ti–N(4) | 1.732(2) |
| Ti–N(2) | 2.080(2) | Ti–N(5) | 2.221(3) |
| Ti–N(3) | 2.408(2) | Ti–N(6) | 2.192(3) |
| N(4)–Ti–N(1) | 106.7(1) | N(4)–Ti–N(2) | 105.3(1) |
| N(2)–Ti–N(1) | 147.6(1) | N(4)–Ti–N(5) | 90.3(1) |
| N(2)–Ti–N(5) | 90.9(1) | N(1)–Ti–N(5) | 150.8(1) |
| N(4)–Ti–N(3) | 177.0(1) | N(6)–Ti–N(3) | 87.5(1) |
| C(41)–N(4)–Ti | 173.6(2) | N(4)–Ti–N(2) | 105.3(1) |

product retains the generated dimethylamine as donor ligands in a mutually trans arrangement (Figure 2, Table 1). The labile dimethylamines are both cis to the reactive imido bond. Consequently, dimethylamine loss exposes the reactive functional group to substrate.

Bergman and co-workers showed that Group-4 imido complexes were the key intermediate in alkyne hydroamination by zirconocene.¹⁹ The observation that titanium with a dpma ancillary ligand has a propensity to stabilize imido ligands, in association with the labile ligands adjacent to the reactive multiple-bond functionality, led us to investigate similar catalyses by the titanium dpma system.

The labile dimethylamine ligands of **2** are readily removed on trituration with various noncoordinating solvents, e.g., toluene, to produce a μ -imido dimer $[\text{Ti}(\text{NPh})(\text{dpma})]_2$ (**3**) with some interesting structural features in the solid state (Figure 3, Table 2). The molecule has one titanium bearing a dpma in a *fac*-arrangement with relatively short Ti–N(imido) bond distances of 1.843(2) and 1.890(2) Å. The cohabitant titanium center has a dpma with a *mer*-arrangement and much longer Ti–N(imido) bond distances of 1.915(2) and 1.993(2) Å. The phenyl groups of the imido ligands both lean toward the titanium with the *mer*-dpma, and the *ipso*-carbon of one phenyl, the one anti to the dpma methyl, has a close contact with a Ti–C distance of 2.477(3) Å. From this, it appears that the titanium center is electron-deficient and is seeking out additional intramolecular interactions in an attempt to sate that deficiency. The dimer **3**, while unsymmetrical in the solid state, exhibits one set of resonances for the dpma and phenyl groups by NMR in fluid solution, presumably due to rapid exchange processes relative to that time scale.

Reactions with donors lead to cleavage of dimeric **3** to terminal imido compounds (eq 3). For example, treatment of the dimer with DME or 4,4'-di-*tert*-butyl-2,2'-bipyridine (Bu^t -

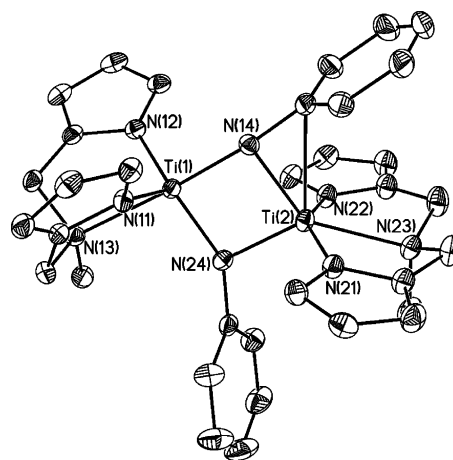
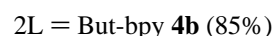
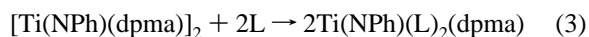


Figure 3. ORTEP representation for the structure of $[\text{Ti}(\text{NPh})(\text{dpma})]_2$ (**3**) from X-ray diffraction. Ellipsoids are at the 25% probability level.

Table 2. Selected Bond Distances (Å) and Angles (deg) from the X-ray Diffraction Study on $[\text{Ti}(\text{NPh})(\text{dpma})]_2$ (**3**)

| | | | |
|-------------------|----------|--------------------|----------|
| Ti(1)–N(11) | 2.005(2) | Ti(2)–N(21) | 2.016(2) |
| Ti(1)–N(13) | 2.310(2) | Ti(2)–N(22) | 2.017(2) |
| Ti(1)–N(12) | 2.038(2) | Ti(2)–N(23) | 2.275(2) |
| Ti(1)–N(14) | 1.843(2) | Ti(2)–N(24) | 1.915(2) |
| Ti(1)–N(24) | 1.890(2) | Ti(2)–N(14) | 1.993(2) |
| | | Ti(2)–C(141) | 2.477(3) |
| N(21)–Ti(2)–N(21) | 148.5(1) | C(141)–N(14)–Ti(1) | 174.0(2) |
| N(11)–Ti(1)–N(12) | 120.3(1) | C(241)–N(24)–Ti(1) | 113.1(2) |
| Ti(1)–N(14)–Ti(2) | 93.9(1) | Ti(1)–N(24)–Ti(2) | 94.9(1) |

bpy) results in formation of $\text{Ti}(\text{NPh})(\text{DME})(\text{dpma})$ (**4a**) and $\text{Ti}(\text{NPh})(\text{Bu}^t\text{-bpy})(\text{dpma})$ (**4b**), respectively.



The investigation of hydroamination with $\text{Ti}(\text{NMe}_2)_2(\text{dpma})$ (**1**), $\text{Ti}(\text{NPh})(\text{dpma})(\text{NHMe}_2)_2$ (**2**), or $[\text{Ti}(\text{NPh})(\text{dpma})]_2$ (**3**) added as catalyst led to the same observed rate constant. In other words, all three species, including the imido dimer, are kinetically competent to be involved under the catalytic conditions.

Synthesis and Reactivity of Hydrazido(1-) and Hydrazido(2-) Titanium dpma Complexes. Only a few titanium complexes bearing multiple hydrazido(1-) ligands have been fully characterized.^{13b,s,t} For example, Leigh and co-workers reported the bis[η^2 -hydrazido(1-)] complex of titanium $\text{Ti}(\text{NMeNMe}_2)_2\text{-Cl}_2$ synthesized from trimethylhydrazine and titanium chloride. As shown in Scheme 2, treatment of a room-temperature solution of $\text{Ti}(\text{NMe}_2)_2(\text{dpma})$ (**1**) with excess 1-aminopiperidine resulted in the generation of an unusual bis[η^2 -hydrazido(1-)] complex $\text{Ti}(\text{NHNC}_5\text{H}_{10})_2(\text{dpma})$ (**5**). Seven-coordinate **5** was readily purified and isolated in 67% yield as yellow microcrystals.

The solid-state structure of **5** determined by X-ray diffraction is shown in Figure 4. The complex exhibits a pseudo-pentagonal bipyramidal arrangement of ligands with two pyrrolyl rings occupying the axial positions. Distances and angles (Table 3) involving the dpma ligand are typical for titanium. Metrical data for **5**, such as $\text{N}_\alpha\text{-Ti}$ distances and angles internal to the

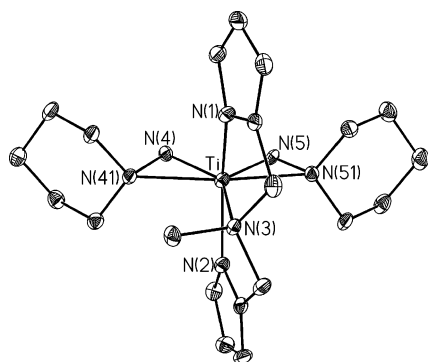


Figure 4. ORTEP representation for the structure of $\text{Ti}(\text{NHNC}_5\text{H}_{10})_2(\text{dpma})$ (**5**) from X-ray diffraction. Ellipsoids are at the 25% probability level.

Scheme 2. Reactions of $\text{Ti}(\text{NMe}_2)_2(\text{dpma})$ (**1**) with 1,1-Dialkylhydrazines

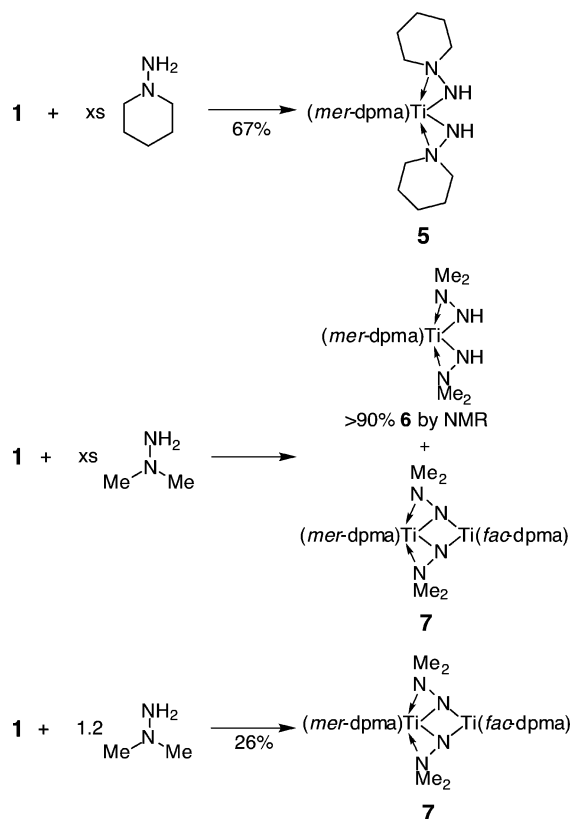


Table 3. Selected Bond Distances (Å) and Angles (deg) from the X-ray Diffraction Study on $\text{Ti}(\text{NHNC}_5\text{H}_{10})_2(\text{dpma})$ (**5**)

| | | | |
|---------------|------------|---------------|------------|
| Ti–N(4) | 1.894(3) | Ti–N(41) | 2.221(3) |
| Ti–N(5) | 1.911(3) | Ti–N(51) | 2.192(3) |
| Ti–N(1) | 2.070(3) | N(4)–N(41) | 1.435(4) |
| Ti–N(2) | 2.082(3) | N(5)–N(51) | 1.432(4) |
| Ti–N(3) | 2.321(3) | | |
| Ti–N(4)–N(41) | 82.45(19) | N(5)–Ti–N(2) | 99.88(12) |
| Ti–N(5)–N(51) | 80.50(18) | N(1)–Ti–N(2) | 147.61(13) |
| N(4)–Ti–N(5) | 89.09(12) | N(4)–Ti–N(3) | 138.1(12) |
| N(4)–Ti–N(1) | 100.05(13) | N(5)–Ti–N(3) | 132.37(12) |
| N(5)–Ti–N(1) | 102.22(12) | N(1)–Ti–N(3) | 73.28(11) |
| N(4)–Ti–N(2) | 103.70(13) | N(2)–Ti–N(3) | 74.34(11) |
| Ti–N(41)–N(4) | 57.71(16) | Ti–N(51)–N(5) | 59.34(16) |

hydrazido ligands, are reminiscent of previously reported η^2 -hydrazido(1-) complexes. For example, the $\text{Ti}-\text{N}_\beta-\text{N}_\alpha$ angles are significantly smaller at $57.7(2)^\circ$ and $59.3(2)^\circ$ than the $\text{Ti}-\text{N}_\alpha-\text{N}_\beta$ angles of $82.4(2)^\circ$ and $80.5(2)^\circ$.

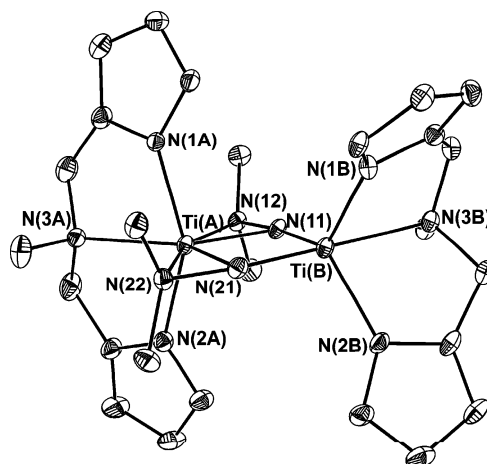
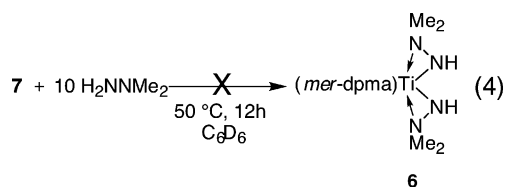


Figure 5. ORTEP representation of the structure of $[\text{Ti}(\text{NNMe}_2)(\text{dpma})]_2$ (**7**) from X-ray diffraction. Ellipsoids are at the 25% probability level.

Treatment of $\text{Ti}(\text{NMe}_2)_2(\text{dpma})$ (**1**) with excess 1,1-dimethylhydrazine results in the formation of two compounds (Scheme 2). The major product is bis[η^2 -hydrazido(1-)] $\text{Ti}(\text{NHNMe}_2)_2(\text{dpma})$ (**6**) analogous to **5**, which has been characterized spectroscopically. A second product of bis[μ : η^1, η^2 -hydrazido(2-)] containing $[\text{Ti}(\text{NNMe}_2)(\text{dpma})]_2$ (**7**) is consistently present in samples of **6** due to loss of H_2NNMe_2 and dimerization. The dimer could be prepared in pure form by addition of a slight excess of H_2NNMe_2 to **1** followed by repeated crystallization. The structure of **7** determined by X-ray diffraction, which bears many features in common with the structure of **3**, is shown in Figure 5. The complex contains one seven-coordinate titanium center and one five-coordinate titanium. The seven-coordinate metal center, Ti(A), bears a *mer*-dpma ligand and is structurally similar to **5**. The five-coordinate metal center, Ti(B), bears a *fac*-dpma and is structurally similar to **1**.²³ Other bridging hydrazido(2-) complexes exhibit this unsymmetrical bridging structure, such as $[\text{ZrCp}_2(\text{NNPh}_2)]_2$ reported by Walsh and Bergman.⁷

Bis(hydrazido) **6** can be prepared in >90% purity, as determined by NMR spectroscopy, through the rapid addition of a large excess of 1,1-dimethylhydrazine to a room-temperature ethereal solution of **1** (Scheme 2). The dimerization is apparently irreversible as addition of 10 equiv of H_2NNMe_2 to a pure sample of dimeric **7** did not afford amounts of monomeric **6** detectable by ^1H NMR, even after heating at 50°C for 12 h (eq 4).



A terminal hydrazido(2-) was not obtained on addition of DME, pyridine, or 4,4'-di-*tert*-butyl-2,2'-bipyridine to bis[μ : η^1, η^2 -hydrazido(2-)] **7**. Fortunately, terminal hydrazido(2-) complexes are available if $\text{Bu}^t\text{-bpy}$ is added prior to addition of 1,1-dimethylhydrazine (Scheme 3). Pseudo-octahedral

(23) Harris, S. A.; Ciszewski, J. T.; Odom, A. L. *Inorg. Chem.* **2001**, *40*, 1987–1988.

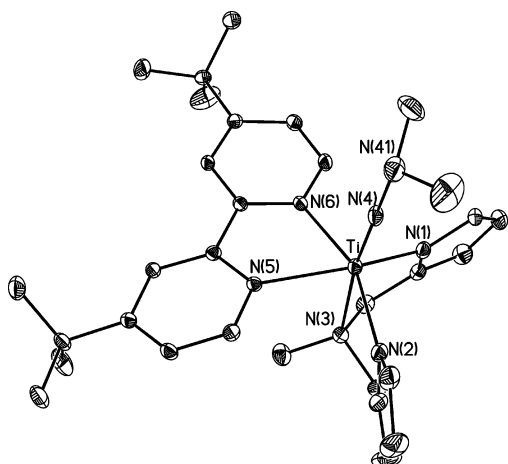
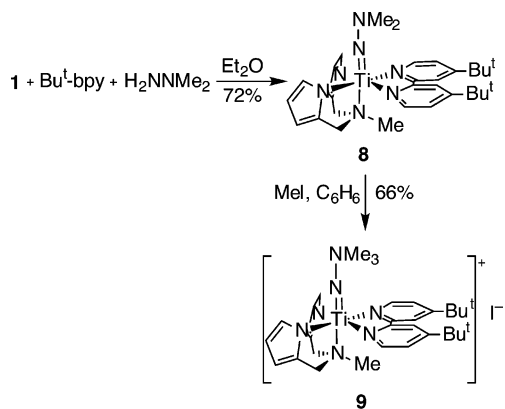


Figure 6. ORTEP representation for the structure of $\text{Ti}(\text{NNMe}_2)(\text{Bu}^t\text{-bpy})(\text{dpma})$ (**8**) from X-ray diffraction with 25% ellipsoids.

Scheme 3. Synthesis of Terminal Hydrazido(2-) Titanium Complexes



$\text{Ti}(\text{NNMe}_2)(\text{Bu}^t\text{-bpy})(\text{dpma})$ (**8**) is prepared by treating **1** with $\text{Bu}^t\text{-bpy}$ followed by 1 equiv of H_2NNMe_2 .

The terminal hydrazido(2-) complex $\text{Ti}(\text{NNMe}_2)(\text{Bu}^t\text{-bpy})(\text{dpma})$ (**8**) was characterized by X-ray diffraction (Figure 6).²⁴ One interesting feature of the structure is the highly pyramidalized β -nitrogen of the hydrazido(2-). The angles around N(41) add to $337(1)^\circ$, only slightly larger than expected for a tetrahedral nitrogen. The pyramidal β -nitrogen suggests that the contribution from the isodiazene resonance form (Chart 1) is only modest. However, the significance of the interaction between the two nitrogens of the hydrazido(2-) group may be better told by the N(4)–N(41) distance of $1.388(4)$ Å, which is slightly shorter than a typical N–N single bond distance (see the structure of $[\text{Ti}(\text{NNMe}_3)(\text{Bu}^t\text{-bpy})(\text{dpma})]^+$ (**9**) below). The hydrazido(2-) ligand is linear with a Ti–N(4)–N(41) angle of $177.3(2)^\circ$.

For comparison with **8**, the imido complex $\text{Ti}(\text{NPh})(\text{Bu}^t\text{-bpy})(\text{dpma})$ (**4b**), which bears the same ancillary ligands as **8**, was

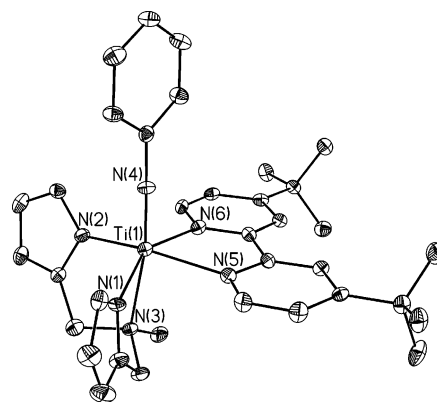


Figure 7. ORTEP representation of the structure of $\text{Ti}(\text{NPh})(\text{Bu}^t\text{-bpy})(\text{dpma})$ (**4b**) from X-ray diffraction. Ellipsoids are at the 25% probability level.

Table 4. Selected Bond Distances (Å) and Angles (deg) from the X-ray Diffraction Study on $[\text{Ti}(\text{NNMe}_2)(\text{dpma})]_2$ (**7**)

| | | | |
|-------------------|------------|-------------------|------------|
| Ti(A)–N(11) | 1.947(4) | Ti(B)–N(11) | 1.837(4) |
| Ti(A)–N(21) | 1.972(4) | Ti(B)–N(21) | 1.836(4) |
| Ti(A)–N(12) | 2.185(4) | Ti(B)–N(1B) | 2.019(4) |
| Ti(A)–N(22) | 2.202(4) | Ti(B)–N(2B) | 2.016(4) |
| Ti(A)–N(1A) | 2.058(4) | Ti(B)–N(3B) | 2.303(4) |
| Ti(A)–N(2A) | 2.056(5) | Ti(A)–N(3A) | 2.299(4) |
| N(21)–Ti(B)–N(11) | 90.66(19) | N(12)–N(11)–Ti(B) | 171.9(4) |
| N(11)–Ti(A)–N(21) | 83.59(18) | N(12)–N(11)–Ti(A) | 79.5(3) |
| N(11)–Ti(A)–N(22) | 122.48(17) | N(22)–N(21)–Ti(B) | 171.8(3) |
| N(12)–Ti(A)–N(22) | 161.50(16) | N(22)–N(21)–Ti(A) | 79.4(3) |
| N(2B)–Ti(B)–N(1B) | 113.12(18) | N(2A)–Ti(A)–N(1A) | 149.34(18) |

Table 5. Selected Bond Distances (Å) and Angles (deg) from the X-ray Diffraction Study on $\text{Ti}(\text{NNMe}_2)(\text{Bu}^t\text{-bpy})(\text{dpma})$ (**8**)

| | | | |
|---------------|----------|--------------|----------|
| Ti–N(4) | 1.708(3) | Ti–N(1) | 2.069(3) |
| Ti–N(2) | 2.064(3) | Ti–N(3) | 2.415(3) |
| Ti–N(6) | 2.242(3) | Ti–N(5) | 2.238(3) |
| N(4)–N(41) | 1.388(4) | | |
| N(4)–Ti–N(2) | 101.1(1) | N(4)–Ti–N(1) | 100.0(1) |
| N(2)–Ti–N(1) | 103.6(1) | N(4)–Ti–N(5) | 101.9(1) |
| N(2)–Ti–N(5) | 90.9(1) | N(1)–Ti–N(5) | 150.8(1) |
| N(4)–Ti–N(3) | 173.2(1) | N(6)–Ti–N(3) | 86.0(1) |
| N(41)–N(4)–Ti | 177.3(2) | | |

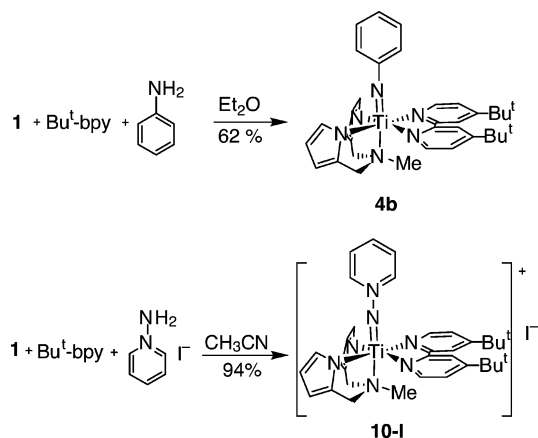
Table 6. Selected Bond Distances (Å) and Angles (deg) from the X-ray Diffraction Study on $\text{Ti}(\text{NPh})(\text{Bu}^t\text{-bpy})(\text{dpma})$ (**4b**)

| | | | |
|------------------|----------|-----------------|----------|
| Ti(1)–N(4) | 1.721(6) | Ti(1)–N(1) | 2.055(6) |
| Ti(1)–N(2) | 2.036(6) | Ti(1)–N(6) | 2.227(6) |
| Ti(1)–N(5) | 2.230(6) | Ti(1)–N(3) | 2.408(6) |
| N(4)–Ti(1)–N(2) | 97.9(3) | N(4)–Ti(1)–N(1) | 103.7(3) |
| N(2)–Ti(1)–N(6) | 92.6(2) | N(2)–Ti(1)–N(1) | 104.2(3) |
| N(4)–Ti(1)–N(6) | 96.9(3) | N(1)–Ti(1)–N(6) | 151.2(2) |
| N(4)–Ti(1)–N(5) | 96.9(3) | N(4)–Ti(1)–N(3) | 171.7(3) |
| C(40)–N(4)–Ti(1) | 171.9(6) | | |

structurally characterized (Figure 7, Table 6). The compound is available from the dimer (eq 3) or directly by addition of aniline and $\text{Bu}^t\text{-bpy}$ to $\text{Ti}(\text{NMe}_2)_2(\text{dpma})$ (**1**) as shown in Scheme 4. The titanium–imido bond distance of $1.721(6)$ Å is typical for this functional group and the same within error as the Ti–N multiple bond in **8**.

We are beginning to probe the effects of substituents on Ti–N bonding in terminal hydrazido(2-) complexes, a feature that may be of paramount importance in designing and understanding successful catalysts for hydrazine hydroamination. The terminal

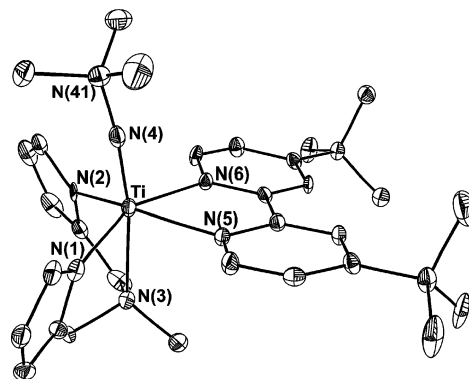
(24) No terminal titanium hydrazido(2-) complexes are found in the latest Cambridge Structural Database at the time of this writing. For examples of structurally characterized terminal hydrazido(2-) compounds of the Group-5 elements, see: (a) Veith, M. *Angew. Chem., Int. Ed. Engl.* **1976**, *15*, 387. (b) Green, M. L. H.; James, J. T.; Chernega, A. N. *J. Chem. Soc., Dalton Trans.* **1997**, 1719. (c) Davies, S. C.; Hughes, D. L.; Janas, Z.; Jerzykiewicz, L.; Richards, R. L.; Sanders, J. R.; Sobota, P. *Chem. Commun.* **1997**, 1261. (d) Davies, S. C.; Hughes, D. L.; Janas, Z.; Jerzykiewicz, L. B.; Richards, R. L.; Sanders, J. R.; Silverston, J. E.; Sobota, P. *Inorg. Chem.* **2000**, *39*, 3485. (e) Green, M. L. H.; James, J. T.; Saunders, J. F.; Souter, J. *J. Chem. Soc., Dalton Trans.* **1997**, 1281. There are many structurally characterized examples of terminal hydrazido(2-) complexes for molybdenum and tungsten.

Scheme 4. Synthesis of Terminal Imido and Pyridinium Imido Titanium Complexes

hydrazido(2-) complexes exhibit a relatively low-energy transition in their absorption spectra that is related to the lone pair on the β -nitrogen. For **8**, the transition is at 547 nm with an absorption coefficient of $1100 \text{ M}^{-1} \text{ cm}^{-1}$. The low-energy absorption results in a dark blue color for **8**, which is quite unusual for a titanium(IV) complex. For example, imido complex **4b** with a very similar ligand set is pale yellow. A study to detail the electronic structure of these metal–ligand multiple-bond complexes and its possible relevance to hydrazido(2-) reactivity is underway.

Even though the isodiazeno resonance form (Chart 1) will participate, **8** is expected to bear a functional group more closely resembling a hydrazido(2-) (vide supra). Considering the two resonance forms may differ significantly in nucleophilicity of N_β , we investigated the reaction of **8** with an electrophile—methyl iodide (Scheme 3). The *N*-trimethylammonium imido complex $[\text{Ti}(\text{NNMe}_3)(\text{Bu}^t\text{-bpy})(\text{dpma})]\text{I}$ (**9**) was prepared, the structure of which is shown in Figure 8.²⁵ The Ti–N(4)–N(41) bond angle in **9** is $173.2(7)^\circ$ (Table 7). This linearity has been noted in all of the structurally characterized *N*-ammonium imido complexes, whether the β -nitrogen is sp^2 or sp^3 hybridized. One of the few other *N*-ammonium imido compounds to be analyzed by X-ray diffraction where the β -nitrogen is sp^3 -hybridized is $[\text{MoCp}^*\text{Me}_3(\text{NNMe}_3)][\text{OTf}]$ prepared by Vale and Schrock.^{25d} The N–N bond distance in **9** is $1.429(13) \text{ \AA}$; the N–N bond distance in $[\text{MoCp}^*\text{Me}_3(\text{NNMe}_3)]^+$ is $1.426(5) \text{ \AA}$, which is very similar to the typical N–N single-bond length of 1.451 \AA .²⁶ In addition, the Ti–N multiple bond measures $1.702(10) \text{ \AA}$, which is in the typical titanium–nitrogen double to triple bond range.

(25) A few complexes with a metal–nitrogen multiple bond bearing a cationic nitrogen of the type $\text{M}=\text{N}-\text{NR}_3$ are known. They have been given the moniker “hydrazidium” previously, which misleadingly has the “ium” ending for a ligand with an overall negative charge. Consequently, we chose an alternative nomenclature derived from *N*-ammonium imido. The only *N*-ammonium imido titanium complexes in the literature are pyridinium imido derivatives, see: (a) Retbøll, M.; Ishii, Y.; Hidai, M. *Organometallics* **1999**, *18*, 150–155. For ammonium imido complexes of other transition metals, see: (b) Ishii, Y.; Tokunaga, S.; Seino, H.; Hidai, M. *Inorg. Chem.* **1999**, *38*, 2489–2496. (c) Ishino, H.; Tokunaga, S.; Seino, H.; Ishii, Y.; Hidai, M. *Inorg. Chem.* **1999**, *38*, 2489–2496. (d) Vale, M. G.; Schrock, R. R. *Inorg. Chem.* **1993**, *32*, 2767–2772. (e) Glassman, T. E.; Vale, M. G.; Schrock, R. R. *J. Am. Chem. Soc.* **1992**, *114*, 8098–8109. (f) Galindo, A.; Hills, A.; Hughes, D. L.; Richards, R. L.; Hughes, M.; Mason, J. *J. Chem. Soc., Dalton Trans.* **1990**, 283–288. (g) Glassman, T. E.; Vale, M. G.; Schrock, R. R. *J. Am. Chem. Soc.* **1992**, *114*, 8098–8109. (h) Wagenknecht, P. S.; Norton, J. R. *J. Am. Chem. Soc.* **1995**, *117*, 1841. (i) Seino, H.; Ishii, Y.; Sasagawa, T.; Hidai, M. *J. Am. Chem. Soc.* **1995**, *117*, 12181–12193. (j) Ishii, Y.; Tokunaga, S.; Seino, H.; Hidai, M. *Inorg. Chem.* **1996**, *35*, 5118–5119.

**Figure 8.** ORTEP representation of the structure of $[\text{Ti}(\text{NNMe}_3)(\text{Bu}^t\text{-bpy})(\text{dpma})]\text{I}$ (**9**) from X-ray diffraction. Anion is not shown. Ellipsoids are at the 25% probability level.**Table 7.** Selected Bond Distances (\AA) and Angles (deg) from the X-ray Diffraction Study on $[\text{Ti}(\text{NNMe}_3)(\text{Bu}^t\text{-bpy})(\text{dpma})]\text{I}$ (**9**)

| | | | |
|---------------|-----------|--------------|-----------|
| Ti–N(4) | 1.702(10) | Ti–N(1) | 2.041(9) |
| Ti–N(2) | 2.052(8) | Ti–N(6) | 2.230(8) |
| Ti–N(5) | 2.221(8) | Ti–N(3) | 2.349(14) |
| N(4)–N(41) | 1.429(13) | | |
| N(4)–Ti–N(2) | 99.6(4) | N(4)–Ti–N(1) | 98.9(4) |
| N(2)–Ti–N(6) | 86.4(3) | N(2)–Ti–N(1) | 105.2(3) |
| N(4)–Ti–N(6) | 100.5(4) | N(1)–Ti–N(6) | 155.4(3) |
| N(4)–Ti–N(5) | 97.2(4) | N(4)–Ti–N(3) | 170.8(4) |
| N(41)–N(4)–Ti | 173.2(7) | | |

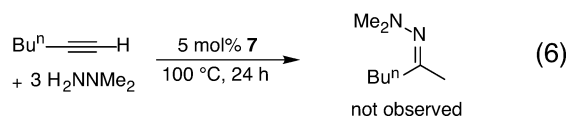
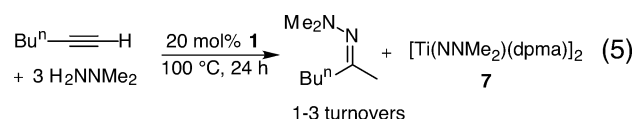
The N–N bond distance in **9** is 0.06 \AA longer than in hydrazido(2-) **8**, suggesting a change in N–N multiple-bond character. On methylation of the lone pair, the blue complex **8** becomes the pale yellow of the ammonium imido, also signifying a significant change in electronic structure.

As shown in Scheme 4, *N*-pyridinium imido complexes^{25a} are readily accessed using a transamination route similar to the hydrazido(2-) syntheses. Addition of 1-aminopyridinium iodide to a solution of $\text{Ti}(\text{NMe}_2)_2(\text{dpma})$ (**1**) and $\text{Bu}^t\text{-bpy}$ in acetonitrile results in the formation of *N*-pyridinium imido $[\text{Ti}(\text{N}-\text{NC}_5\text{H}_5)(\text{Bu}^t\text{-bpy})(\text{dpma})]\text{I}$ (**10-I**) in 94% recrystallized yield. While **10-I** has not been structurally characterized, its spectroscopic and chemical properties are consistent with the salt formulation. For example, the iodide is readily exchanged with other counterions through reaction with AgOTf and AgBF_4 to form $[\text{Ti}(\text{N}-\text{NC}_5\text{H}_5)(\text{Bu}^t\text{-bpy})(\text{dpma})]\text{OTf}$ (**10-OTf**) and $[\text{Ti}(\text{N}-\text{NC}_5\text{H}_5)(\text{Bu}^t\text{-bpy})(\text{dpma})]\text{BF}_4$ (**10-BF₄**), respectively. Also in support of the salt formulation, **10-OTf** and **10-BF₄** have absorption spectra very similar to **10-I**. Interestingly, **10-I** exhibits an emission with a maximum at 469 nm on excitation at 303 nm. Investigating the nature of this emission was the initial impetus behind the synthesis of **10-OTf** and **10-BF₄**. While **10-OTf** and **10-BF₄** have an absorption spectrum similar to **10-I**, no emission is observed for the complexes. In addition, $[\text{Ti}(\text{NNMe}_3)(\text{Bu}^t\text{-bpy})(\text{dpma})]\text{I}$ (**9**) does not emit, which suggests that *bpy* is not the acceptor for the charge transfer. Consequently, the transition leading to emission is likely due to an iodide to pyridinium imido charge transfer. Consistent with this assertion, 1-aminopyridinium iodide also emits under the same conditions, albeit at a substantially shifted wavelength from the emission of **10-I**.

(26) Gordon, A. J.; Ford, R. A. *The Chemist's Companion: A Handbook of Practical Data, Techniques, and References*; John Wiley & Sons: New York, 1972.

Concluding Comments and Relevance to Hydroamination

For successful hydroamination activity, it appears necessary for the titanium catalyst to access terminal multiple-bond species. Reaction of $\text{Ti}(\text{NMe}_2)_2(\text{dpma})$ (**1**) with primary amines, e.g., aniline, results in the formation of isolable dimeric $[\text{Ti}(\mu\text{-NPh})(\text{dpma})_2]$ (**3**), which readily reacts with many different donor ligands, such as DME and $\text{Bu}^t\text{-bpy}$, to provide monomeric, terminal imido titanium complexes **4**. Examination of the reactions between **1** and H_2NNMe_2 led to the synthesis and isolation of dimeric hydrazido(2-) $[\text{Ti}(\text{NNMe}_2)(\text{dpma})_2]$ (**7**). Because neither 1,1-dimethylhydrazine nor $\text{Bu}^t\text{-bpy}$ can prompt conversion of dimeric **7** to a monomeric species, it is postulated that the formation of **7** is one cause for inefficient alkyne hydroamination catalysis by **1** with dimethylhydrazine.¹⁸ Since terminal hydrazido(2-) complexes are likely necessary for hydroamination activity,¹⁹ catalysis terminates on conversion of the available titanium to dimeric **7**. Indeed, reexamination by ^1H NMR spectroscopy of hydroamination reactions with **1** as catalyst confirms the presence of **7** (eq 5). Attempts to use dimeric **7** or monomeric bis[dimethylhydrazido(1-)] **6** as catalyst provided no hydroamination product (eq 6).



Consequently, it is apparent that the additional dative interactions between the β -nitrogens of the hydrazido ligands and titanium limit the catalytic activity. To destabilize these dative interactions and allow conversion of the dimeric hydrazido(2-) complex to terminal hydrazido species, one can alter the ancillary ligand set to add more bulk, make the metal center more electron-rich, or both. The strategy behind the design of the catalyst in Scheme 1 was to increase the coordination number by one and add an additional donor amine. The dpma ligand can be regarded as an X_2L ancillary ligand;²⁷ whereas, the more active $\text{Ti}(\text{NMe}_2)_2(\text{dap})_2$ possesses an X_2L_2 ancillary ligand set. It is the desire to weaken the dative interactions in μ -hydrazido(2-) intermediates that led to the design of the successful hydrazine hydroamination catalyst shown in Scheme 1.²⁸

Experimental Section

General Considerations. All manipulations of air-sensitive compounds were carried out in an MBraun drybox under a purified nitrogen atmosphere. Anhydrous ether was purchased from Columbus Chemical Industries Inc. and freshly distilled from purple sodium benzophenone ketyl. Toluene was purchased from Spectrum Chemical Mfg. Corp. and purified by refluxing over molten sodium under nitrogen for at least 2 days. Pentane (Spectrum Chemical Mfg. Corp.), tetrahydrofuran

(JADE Scientific), and benzene (EM Science) were distilled from purple sodium benzophenone ketyl. Dichloromethane (EM Science) and acetonitrile (Spectrum Chemical) were distilled from calcium hydride. Deuterated solvents were dried over purple sodium benzophenone ketyl (C_6D_6) or phosphoric anhydride (CDCl_3) and distilled under nitrogen. ^1H and ^{13}C spectra were recorded on Inova-300 and VXR-500 spectrometers. ^1H and ^{13}C assignments were confirmed when necessary with the use of two-dimensional ^1H – ^1H and ^{13}C – ^1H correlation NMR experiments. All spectra were referenced internally to residual protio-solvent (^1H) or solvent (^{13}C) resonances. Chemical shifts are quoted in ppm and coupling constants in Hz. $\text{H}_2\text{dpma}^{15}$ and $\text{Ti}(\text{NMe}_2)_2(\text{dpma})$ (**1**)²³ were prepared as previously described.

General Considerations for X-ray Diffraction. Crystals grown from concentrated solutions at $-35\text{ }^\circ\text{C}$ quickly were moved from a scintillation vial to a microscope slide containing Paratone N. Samples were selected and mounted on a glass fiber in wax and Paratone. The data collections were carried out at a sample temperature of 173 K on a Bruker AXS platform three-circle goniometer with a CCD detector. The data were processed and reduced utilizing the program SAINT-PLUS supplied by Bruker AXS. The structures were solved by direct methods (SHELXTL v5.1, Bruker AXS) in conjunction with standard difference Fourier techniques.

Collection of Emission Spectra. Emission spectra were collected on a Fluorolog-3 spectrofluorometer made by the Spex Fluorescence Group of Jobin Yvon Horiba equipped with a 450 W Xe excitation lamp and a 1527 PMT. The spectra were taken in THF at room temperature. Sample spectra can be found in the Supporting Information.

Ti(NPh)(NHMe₂)(dpma) (2). To a frozen solution of $\text{Ti}(\text{NMe}_2)_2(\text{dpma})$ (**1**) (323 mg, 1.00 mmol) in CH_2Cl_2 (5 mL) was added PhNH_2 (91 μL , 1.00 mmol). The reaction mixture was allowed to stand at $-35\text{ }^\circ\text{C}$ for 24 h. Onto the resulting red solution was layered 2 mL of pentane. The vial was then stored at $-35\text{ }^\circ\text{C}$, which yielded **2** as a red crystalline solid in 94% yield (0.391 g). ^1H NMR (300 MHz, C_6D_6): $\delta = 7.88$ (2 H, d, $J = 1$ Hz, 5- $\text{C}_4\text{H}_3\text{N}$), 7.23–7.11 (4 H, m, 2,3- $\text{C}_6\text{H}_5\text{N}$), 6.78 (1 H, m, 4- $\text{C}_6\text{H}_5\text{N}$), 6.62 (2 H, dd, 4- $\text{C}_4\text{H}_3\text{N}$), 6.20 (2 H, d, $J = 2$ Hz, 3- $\text{C}_4\text{H}_3\text{N}$), 3.15 (4 H, s, $\text{C}_4\text{H}_3\text{NCH}_2\text{N}$), 2.04 (12 H, br s, $\text{HN}(\text{CH}_3)_2$), 1.68 (3 H, s, $\text{C}_4\text{H}_3\text{NCH}_2\text{NCH}_3$), 1.4 (2 H, br s, HNMe_2). $^{13}\text{C}\{^1\text{H}\}$ NMR (300 MHz, CDCl_3): $\delta = 158.7$ (1- $\text{C}_6\text{H}_5\text{N}$), 137.6 (2- $\text{C}_4\text{H}_3\text{N}$), 130.4 (5- $\text{C}_4\text{H}_3\text{N}$), 128.5 (3- $\text{C}_6\text{H}_5\text{N}$), 124.9 (4- $\text{C}_6\text{H}_5\text{N}$), 120.3 (2- $\text{C}_6\text{H}_5\text{N}$), 107.3 (4- $\text{C}_4\text{H}_3\text{N}$), 102.5 (3- $\text{C}_4\text{H}_3\text{N}$), 60.8 ($\text{C}_4\text{H}_3\text{NCH}_2\text{NCH}_3$), 45.4 ($\text{C}_4\text{H}_3\text{NCH}_2\text{NCH}_3$), 41.9 ($\text{HN}(\text{CH}_3)_2$). Elemental analysis for $\text{C}_{21}\text{H}_{32}\text{N}_6\text{Ti}$, found (calcd): C, 60.28 (60.57); H, 7.81 (7.74); N, 19.97 (20.18).

[Ti(NPh)(dpma)]₂ (3). To a solution of $\text{Ti}(\text{NMe}_2)_2(\text{dpma})$ (**1**) (0.323 g, 1 mmol) in toluene (5 mL) cooled to $-50\text{ }^\circ\text{C}$ was added a solution of PhNH_2 (182 μL , 2 mmol) in toluene (2 mL). The reaction mixture was stirred at room temperature for 12 h, after which time volatiles were removed under reduced pressure. The solid was dissolved in CH_2Cl_2 and recrystallized at $-35\text{ }^\circ\text{C}$, yielding 0.323 g (98%) of $[\text{Ti}(\text{dpma})(\text{NPh})_2]$ as a black solid. ^1H NMR (300 MHz, C_6D_6): $\delta = 7.71$ (4 H, d, $J = 1$ Hz, 5- $\text{C}_4\text{H}_3\text{N}$), 6.83–6.43 (4 H, m, 4- $\text{C}_4\text{H}_3\text{N}$, C_6H_5), 6.07 (4 H, d, $J = 2$ Hz, 3- $\text{C}_4\text{H}_3\text{N}$), 3.36 (4 H, d, $J = 14$ Hz, $\text{C}_4\text{H}_3\text{NCH}_2\text{N}$), 3.18 (4 H, d, $J = 14$ Hz, $\text{C}_4\text{H}_3\text{NCH}_2\text{N}$), 1.74 (6 H, s, NCH_3). $^{13}\text{C}\{^1\text{H}\}$ (300 MHz, CDCl_3): 138.0 (2- $\text{C}_4\text{H}_3\text{N}$), 134.1 (1- $\text{C}_6\text{H}_5\text{N}$), 130.2 (5- $\text{C}_4\text{H}_3\text{N}$), 129.5 (5- $\text{C}_4\text{H}_3\text{N}$), 125.8 (4- $\text{C}_6\text{H}_5\text{N}$), 122.7 (2- $\text{C}_6\text{H}_5\text{N}$), 108.5 (4- $\text{C}_4\text{H}_3\text{N}$), 103.0 (3- $\text{C}_4\text{H}_3\text{N}$), 59.8 ($\text{C}_4\text{H}_3\text{NCH}_2\text{N}$), 45.4 (NCH_3). Elemental analysis for $\text{C}_{34}\text{H}_{36}\text{N}_8\text{Ti}_2$: found (calcd) C, 61.85 (62.20); H, 5.58 (5.53); N, 17.07 (17.07).

Ti(NPh)(DME)(dpma) (4a). To a 250 mL round-bottom flask equipped with a stir bar was added dark red $[\text{Ti}(\text{NPh})(\text{dpma})_2]$ (424 mg, 0.65 mmol) and 40 mL of DME. After stirring at room temperature for 4 h, volatiles of the reaction mixture were removed in vacuo to yield a dark orange solid. The solid was recrystallized from CH_2Cl_2 /pentane at $-35\text{ }^\circ\text{C}$, which provided 253 mg of product. Yield: 47%. ^1H NMR (300 MHz, CDCl_3): $\delta = 7.34$ (2 H, s, 5- $\text{C}_4\text{H}_3\text{N}$), 7.28 (2 H, m, 2- C_6H_5), 7.18 (2 H, m, 3- C_6H_5), 6.96 (1 H, m, 4- C_6H_5), 6.15 (2 H,

(27) Green, M. L. H. *J. Organomet. Chem.* **1995**, *500*, 127–148.

(28) Investigation of other ancillaries for hydrazine hydroamination led to the synthesis of $\text{Ti}(\text{SC}_6\text{F}_5)_2(\text{NMe}_2)_2(\text{NHMe}_2)$, which bears two electron-deficient thiolates, as an alternative hydrazine hydroamination catalyst, see ref 18.

m, 4-C₄H₃N), 5.96 (2 H, s, 3-C₄H₃N), 3.78 (4 H, s, C₄H₃NCH₂N), 3.59 (4 H, d, CH₃OC₂H₄OCH₃), 3.44 (6 H, s, CH₃OC₂H₄OCH₃) 2.22 (3 H, s, NCH₃). ¹³C{¹H} NMR (CDCl₃): δ = 138.1 (2-C₄H₃N), 134.2 (5-C₄H₃N), 130.3 (1-C₆H₅), 129.5 (2-C₆H₅), 129.3 (3-C₆H₅), 125.8 (4-C₆H₅), 108.5 (4-C₄H₃N), 103.0 (3-C₄H₃N), 71.8 (CH₃OC₂H₄OCH₃), 59.8 (C₄H₃NCH₂N), 59.1 (CH₃OC₂H₄OCH₃), 45.4 (C₄H₃NCH₂NCH₃). Elemental analysis for C₂₁H₂₈N₄O₂Ti, found (calcd): C, 60.33 (60.59); H, 6.85 (6.73); N, 13.18 (13.47).

Ti(NPh)(dpma)(Bu^t-bpy) (4b). *Method A:* To a dark red solution of [Ti(NPh)(dpma)]₂ (215 mg, 0.33 mmol) in CH₂Cl₂ (5 mL) was added a solution of Bu^t-bpy in CH₂Cl₂ (3 mL) dropwise. After stirring at room temperature overnight, volatiles of the reaction mixture were removed in vacuo to yield an orange solid. Yield: 335 mg (85%). *Method B:* To a near frozen solution of Ti(NMe₂)₂(dpma) (1) (323 mg, 1.00 mmol) and Bu^t-bpy (268 mg, 1.00 mmol) in Et₂O (10 mL) was added a solution of PhNH₂ (93 mg, 1.00 mmol) in Et₂O (5 mL) dropwise. After stirring at room temperature overnight, volatiles were removed in vacuo to yield an orange solid. The solid was recrystallized from CH₂Cl₂, yielding crystals suitable for X-ray diffraction. Yield: 366 mg (62%). ¹H NMR (300 MHz, CDCl₃): δ = 8.02 (2 H, s, 3,3'-[Bu^t-bpy]), 7.70 (2 H, s, 5-C₄H₃N), 7.45 (2 H, m, 6,6'-[Bu^t-bpy]), 7.38 (2 H, m, 5,5'-[Bu^t-bpy]), 6.89 (2 H, m, 3-C₆H₅), 6.69 (2 H, d, 2-C₆H₅), 6.58 (1 H, m, 4-C₆H₅), 6.26 (2 H, dd, 4-C₄H₃N), 5.94 (2 H, s, 3-C₄H₃N), 3.80 (2 H, d, ²J = 13.7 Hz, C₄H₃NCH₂N), 3.12 (2 H, d, ²J = 13.6 Hz, C₄H₃NCH₂N), 1.52 (3 H, s, C₄H₃NCH₂NCH₃), 1.39 (18 H, s, 4,4'-di-*tert*-butyl). ¹³C-{¹H} NMR (CDCl₃): δ = 164.3 (2,2'-[Bu^t-bpy]), 152.6 (4,4'-[Bu^t-bpy]), 151.6 (6,6'-[Bu^t-bpy]), 136.8 (2-C₄H₃N), 129.8 (5,5'-[Bu^t-bpy]), 127.8 (1,4-C₆H₅), 124.2 (2,3-C₆H₅), 123.7 (5-C₄H₃N), 119.4 (4-C₆H₅), 117.1 (3,3'-[Bu^t-bpy]), 107.3 (4-C₄H₃N), 102.5 (3-C₄H₃N), 58.5 (C₄H₃NCH₂N), 44.5 (C(CH₃)₃-[Bu^t-bpy]), 35.5 (C₄H₃NCH₂NCH₃), 30.3 (C(CH₃)₃-[Bu^t-bpy]). Elemental analysis for C₃₅H₄₂N₆Ti, found (calcd): C, 69.84 (70.58); H, 7.18 (7.06); N, 13.84 (14.13).

Ti(dpma)(NHNC₅H₁₀)₂ (5). To Ti(NMe₂)₂(dpma) (1) (234 mg, 0.72 mmol) in 5 mL of Et₂O was quickly added 1-aminopiperidine (2 mL, 18.5 mmol, 26 equiv). After 1 h, a cloudy orange solution was obtained. The solution was filtered, and the yellow precipitate was washed with ether. The volatiles of the combined filtrates were removed under reduced pressure to yield a yellow solid. The solid was dissolved into CH₂Cl₂ and cooled to -35 °C, providing 210 mg (67%) of yellow microcrystals. Single crystals suitable for X-ray diffraction were grown from a saturated CH₂Cl₂ solution at -35 °C. ¹H NMR (300 MHz, CDCl₃): δ = 7.55 (2 H, s, TiNHNC₅H₁₀), 6.43 (2 H, s, 5-C₄H₃N), 5.88 (2 H, m, 4-C₄H₃N), 5.74 (2 H, m, 3-C₄H₃N), 4.42 (2 H, d, ²J = 13.7 Hz, C₄H₃NCH₂N), 4.04 (2 H, s, ²J = 13.8 Hz, C₄H₃NCH₂N), 2.91 (3 H, s, C₄H₃NCH₂NCH₃), 2.83–2.58 (6 H, m, TiNHNC₅H₁₀), 1.65–1.32 (14 H, m, TiNHNC₅H₁₀). ¹³C{¹H} NMR (CDCl₃): δ = 138.2 (2-C₄H₃N), 126.8 (5-C₄H₃N), 106.8 (4-C₄H₃N), 100.6 (3-C₄H₃N), 62.7 (C₄H₃NCH₂N), 58.3 (C₄H₃NCH₂NCH₃), 24.2 (2-C₅H₁₀N), 23.5 (4-C₅H₁₀N), 22.4 (3-C₅H₁₀N). Elemental analysis for C₂₁H₃₅N₇Ti, found (calcd): C, 58.19 (58.22); H, 7.95 (8.14); N, 22.50 (22.62).

Ti(NHNMe₂)₂(dpma) (6). To an orange solution of Ti(dpma)(NMe₂)₂ (1) (231 mg, 0.71 mmol) in Et₂O (10 mL) was quickly added a solution of H₂NNMe₂ (1.580 g, 26.3 mmol) in 5 mL of Et₂O. After stirring at room temperature for 1 h, volatiles were removed in vacuo to give a yellow solid. Unlike for 5, we were unable to purify the complex due to irreversible formation of dimeric [Ti(μ-NNMe₂)(dpma)]₂ (7) during recrystallization. The complex formed using this preparation was >90% 6 by ¹H NMR. ¹H NMR (300 MHz, CDCl₃) δ = 6.81 (2 H, s, TiHNNMe₂), 6.54 (2 H, s, 5-C₄H₃N), 5.97 (2 H, dd, 4-C₄H₃N), 5.86 (2 H, s, 3-C₄H₃N), 4.40 (2 H, d, ²J = 13.6 Hz, C₄H₃NCH₂N), 4.07 (2 H, d, ²J = 13.7 Hz, C₄H₃NCH₂N), 2.95 (3 H, s, C₄H₃NCH₂NCH₃), 2.64 (6 H, d, TiN(H)N(CH₃)₂), 2.10 (6 H, d, TiNHN(CH₃)₂). ¹³C{¹H} NMR (CDCl₃): δ = 137.9 (2-C₄H₃N), 126.9 (5-C₄H₃N), 106.9 (4-C₄H₃N), 100.7 (3-C₄H₃N), 62.9 (C₄H₃NCH₂N), 51.6 (TiHNNCH₃), 51.0 (TiHNNCH₃), 47.8 (C₄H₃NCH₂NCH₃).

[Ti(μ-NNMe₂)(dpma)]₂ (7). To Ti(NMe₂)₂(dpma) (1) (298.6 mg, 0.92 mmol) in 10 mL of Et₂O cooled to -100 °C was added H₂NNMe₂ (84 μL, 1.10 mmol) in 2 mL of Et₂O dropwise. The mixture was allowed to warm to room temperature and stir for 16 h. The solution was filtered away from a yellow solid, which was recrystallized from CH₂Cl₂ to yield the orange dimer 7 (71 mg, 26%). ¹H NMR (300 MHz, CDCl₃): δ = 7.02 (2 H, s, 5-C₄H₃N), 6.10 (2 H, s, 3-C₄H₃N), 6.07 (2 H, m, 4-C₄H₃N), 5.98 (2 H, s, 5-C₄H₃N), 5.77 (2 H, s, 3-C₄H₃N), 5.75 (2 H, m, 4-C₄H₃N), 4.50 (2 H, d, ²J = 14 Hz, C₄H₃NCH₂N), 4.25 (2 H, d, ²J = 13.7 Hz, C₄H₃NCH₂N), 4.18 (2 H, d, ²J = 13.7 Hz, C₄H₃NCH₂N), 4.01 (2 H, d, ²J = 13.7 Hz, C₄H₃NCH₂N), 3.22 (6 H, s, NNMe₂), 3.20 (3 H, s, C₄H₃NCH₂NCH₃), 3.09 (3 H, s, C₄H₃NCH₂NCH₃), 2.49 (6 H, s, NNMe₂). ¹³C{¹H} NMR (CDCl₃): δ = 138.4 (2-C₄H₃N), 137.5 (2-C₄H₃N), 129.6 (5-C₄H₃N), 127.4 (5-C₄H₃N), 108.1 (4-C₄H₃N), 107.9(4-C₄H₃N), 103.5 (3-C₄H₃N), 101.7 (3-C₄H₃N), 63.0 (C₄H₃NCH₂N), 58.8 (C₄H₃NCH₂N), 52.3 (NNMe₂), 51.9 (NNMe₂), 50.2 (C₄H₃NCH₂NCH₃), 48.7 (C₄H₃NCH₂NCH₃). Elemental analysis for C₂₆H₃₈N₁₀Ti₂, found (calcd): C, 52.74 (53.21); H, 6.58 (6.48); N, 23.32 (23.88).

Ti(dpma)(Bu^t-bpy)(NNMe₂) (8). To Ti(NMe₂)₂(dpma) (1) (1.018 g, 3.15 mmol) and Bu^t-bpy (845 mg, 3.15 mmol) in Et₂O (10 mL) cooled to -100 °C was added H₂NNMe₂ (189 mg, 3.15 mmol) in Et₂O (5 mL) dropwise. After stirring at room temperature overnight, volatiles were removed in vacuo, resulting in a purple solid, which was washed with pentane. Yield: 1.27 g (72%). ¹H NMR (300 MHz, CDCl₃): δ = 8.03 (2 H, s, 3,3'-[Bu^t-bpy]), 7.70 (2 H, s, 5-C₄H₃N), 7.67 (2 H, m, 6,6'-[Bu^t-bpy]), 7.38 (2 H, m, 5,5'-[Bu^t-bpy]), 6.26 (2 H, dd, 4-C₄H₃N), 5.94 (2 H, s, 3-C₄H₃N), 3.72 (2 H, d, ²J = 13.5 Hz, C₄H₃NCH₂N), 3.02 (2 H, d, ²J = 13.4 Hz, C₄H₃NCH₂N), 2.57 (6 H, s, TiNN(CH₃)₂), 1.41 (18 H, s, *tert*-butyl), 1.38 (3 H, s, C₄H₃NCH₂NCH₃). ¹³C{¹H} NMR (CDCl₃): δ = 163.5 (2,2'-[Bu^t-bpy]), 152.2 (4,4'-[Bu^t-bpy]), 151.4 (6,6'-[Bu^t-bpy]), 136.9 (2-C₄H₃N), 131.6 (5,5'-[Bu^t-bpy]), 123.1 (5-C₄H₃N), 117.0 (3,3'-[Bu^t-bpy]), 107.0 (4-C₄H₃N), 102.0 (3-C₄H₃N), 58.4 (C₄H₃NCH₂N), 48.0 (TiNN(CH₃)₂), 44.1 (C₄H₃NCH₂NCH₃), 35.2 (C(CH₃)₃-[Bu^t-bpy]), 30.3 (C(CH₃)₃-[Bu^t-bpy]). Absorption spectrum: λ_{max} = 547 nm, ε = 1100 cm⁻¹ M⁻¹. Elemental analysis for C₃₁H₄₃N₇Ti, found (calcd): C, 66.31 (66.28); H, 7.99 (7.73); N, 17.23 (17.46).

[Ti(dpma)(Bu^t-bpy)(NNMe₂)]I (9). To Ti(dpma)(Bu^t-bpy)(NNMe₂) (8) (700 mg, 1.25 mmol) in benzene (5 mL) at 0 °C was added MeI (78 μL, 1.25 mmol) in benzene (3 mL) dropwise. The solution was allowed to warm and stir after addition. The solution turned from the blue of the starting material to yellow. After being stirred at room temperature overnight, volatiles were removed in vacuo, yielding a yellow solid. Recrystallization from ~3 mL of CH₂Cl₂ at -35 °C provided yellow microcrystals. Yield: 580 mg (66%). Single crystals suitable for X-ray diffraction were grown by cooling a concentrated solution of 9 in CH₂Cl₂. ¹H NMR (300 MHz, d₈-THF): δ = 8.72 (2 H, s, 3,3'-[Bu^t-bpy]), 7.49 (2 H, d, 6,6'-[Bu^t-bpy]), 7.40 (2 H, d, 5-C₄H₃N), 6.99 (2 H, d, 5,5'-[Bu^t-bpy]), 6.05 (2 H, dd, 4-C₄H₃N), 5.84 (2 H, d, 3-C₄H₃N), 3.82 (2 H, d, ²J = 13.7 Hz, C₄H₃NCH₂N), 3.26 (2 H, d, ²J = 13.4 Hz, C₄H₃NCH₂N), 1.72 (9 H, s, TiNN(CH₃)₃), 1.65 (3 H, s, C₄H₃NCH₂NCH₃), 1.45 (18 H, s, C(CH₃)₃-[Bu^t-bpy]). ¹³C{¹H} NMR (d₈-THF): δ = 165.8 (2,2'-[Bu^t-bpy]), 153.9 (4,4'-[Bu^t-bpy]), 150.6 (6,6'-[Bu^t-bpy]), 137.3 (2-C₄H₃N), 132.9 (5,5'-[Bu^t-bpy]), 130.8 (3,3'-[Bu^t-bpy]), 124.8 (5-C₄H₃N), 108.7 (4-C₄H₃N), 103.8 (3-C₄H₃N), 60.3 (TiNN(CH₃)₃), 59.7 (TiNN(CH₃)₃), 45.18 (C(CH₃)₃-[Bu^t-bpy]), 36.5 (C₄H₃NCH₂NCH₃), 30.58 (C(CH₃)₃). Elemental analysis for C₃₂H₄₆N₇ITi, found (calcd): C, 54.93 (54.62); H, 6.77 (6.60); N, 13.46 (13.94).

[Ti(dpma)(Bu^t-bpy)(N-pyridinium imido)]I (10-I). To a near frozen solution of Ti(NMe₂)₂(dpma) (1) (700 mg, 2.16 mmol) and Bu^t-bpy (581 mg, 2.16 mmol) in CH₃CN (10 mL) was added a solution of 1-aminopyridinium iodide (481 mg, 2.16 mmol) in CH₃CN (5 mL) dropwise. The reaction was stirred for 10 h at room temperature. Volatiles were removed in vacuo to give a dark yellow solid. Yield: 1.48 g (94%). Single crystals were grown from CH₃CN by slow evaporation. ¹H NMR (300 MHz, CDCl₃): δ = 8.61 (2 H, m, 6,6'-

[Bu^t-bpy]), 8.39 (2 H, d, 2-C₅H₅N), 7.85 (4 H, m, 5,5'-[Bu^t-bpy] and 3,3'-[Bu^t-bpy]), 7.45 (2H, dd, 3-C₅H₅N), 7.21 (2H, s, 5-C₄H₅N), 7.07 (1 H, dd, 4-C₅H₅N), 6.19 (2 H, dd, 4-C₄H₅N), 6.00 (2 H, d, 3-C₄H₅N), 4.05 (2 H, d, ²J = 13.9 Hz, C₅H₄NCH₂N), 3.45 (2 H, d, ²J = 13.9 Hz, C₅H₄NCH₂N), 1.86 (3 H, s, C₅H₄NCH₂NCH₃), 1.49 (18 H, s, C(CH₃)₃-[Bu^t-bpy]). ¹³C{¹H} NMR (CDCl₃): δ = 166.4 (2,2'-[Bu^t-bpy]), 152.7 (4,4'-[Bu^t-bpy]), 150.7 (6,6'-[Bu^t-bpy]), 141.0 (4-C₅H₅N), 136.8 (2-C₅H₄N), 136.1 (5,5'-[Bu^t-bpy]), 127.8 (5-C₄H₅N), 124.7 (3-C₅H₅N), 119.8 (2-C₅H₅N), 109.0 (4-C₄H₅N), 103.6 (3-C₄H₅N), 59.4 (C₅H₄NCH₂N), 45.7 (C₅H₄NCH₂NCH₃), 35.87 (C(CH₃)₃-[Bu^t-bpy]), 30.3 (C(CH₃)₃-[Bu^t-bpy]). Absorption spectrum: λ_{max} = 346 nm, ε = 12 400 cm⁻¹ M⁻¹. Elemental analysis for C₃₄H₄₂IN₇Ti, found (calcd): C, 56.88 (56.43); H, 5.94 (5.86); N, 13.29 (13.55).

[Ti(dpma)(Bu^t-bpy)(N-pyridinium imido)]OTf (10-OTf). To a suspension of AgOTf (81 mg, 0.31 mmol) in CH₃CN cooled to -100 °C was added a cold solution of [Ti(dpma)(Bu^t-bpy)(N-1-pyridinium)]I (**10-I**) (227 mg, 0.31 mmol) in CH₃CN dropwise. The reaction mixture was allowed to warm to room temperature and stir 16 h. After this, a gray precipitate was filtered away from the yellow-brown solution. The volatiles were removed in vacuo, yielding a brown solid. The solid was recrystallized from CH₃CN at -35 °C, which provided 115 mg (49%) of **10-OTf**. ¹H NMR (300 MHz, CDCl₃): δ = 8.49 (2 H, m, 6,6'-[Bu^t-bpy]), 8.38 (2 H, d, 2-C₅H₅N), 7.78 (2 H, m, 5,5'-[Bu^t-bpy]), 7.66 (2 H, dd, 3,3'-[Bu^t-bpy]), 7.43 (2 H, dd, 3-C₅H₅N), 7.22 (2 H, s, 5-C₄H₅N), 7.04 (2 H, dd, 4-C₅H₅N), 6.20 (2 H, dd, 4-C₄H₅N), 5.95 (2 H, m, 3-C₄H₅N), 3.99 (2 H, d, ²J = 13.9 Hz, C₅H₄NCH₂N), 3.40 (2 H, d, ²J = 13.9 Hz, C₅H₄NCH₂N), 1.85 (3 H, s, C₅H₄NCH₂NCH₃), 1.46 (18 H, s, C(CH₃)₃[Bu^t-bpy]). ¹³C{¹H} NMR (CDCl₃): δ = 166.5 (2,2'-[Bu^t-bpy]), 153.0 (4,4'-[Bu^t-bpy]), 150.5 (6,6'-[Bu^t-bpy]), 141.1 (4-C₅H₅N), 136.8 (2-C₅H₄N), 136.9 (5,5'-[Bu^t-bpy]), 127.9 (5-C₄H₅N), 124.5 (3-C₅H₅N), 119.8 (2-C₅H₅N), 108.9 (4-C₄H₅N), 103.6 (3-C₄H₅N), 59.5 (C₅H₄NCH₂N), 45.7 (C₅H₄NCH₂NCH₃), 35.8 (C(CH₃)₃-[Bu^t-bpy]), 30.2 (C(CH₃)₃-[Bu^t-bpy]). Absorption spectrum: λ_{max} = 347 nm, ε = 19 200 cm⁻¹ M⁻¹. Elemental analysis for TiC₃₅H₄₂N₇SF₃O₃, found (calcd): C, 56.19 (56.32); H, 5.78 (5.63); N, 12.83 (13.14).

[Ti(dpma)(Bu^t-bpy)(N-pyridinium imido)]BF₄ (10-BF₄). To a suspension of AgBF₄ (53.2 mg, 0.27 mmol) in CH₃CN at -100 °C was added a cold solution of [Ti(dpma)(Bu^t-bpy)(N-1-pyridinium)]I (**10-I**) (200 mg, 0.276 mmol) in CH₃CN dropwise. The mixture was allowed to warm to room temperature and stirred for 16 h. The reaction was filtered to remove a gray precipitate from the yellow-brown solution. Volatiles were removed in vacuo, and the resulting solid was recrystallized from CH₃CN at -35 °C, yielding 112 mg (60%) of yellow product. ¹H NMR (300 MHz, CDCl₃): δ = 8.37 (4 H, m, 2-C₅H₅N, 3-C₅H₅N), 7.7 (1 H, m, 4-C₅H₅N), 7.65 (2 H, m, 6,6'-[Bu^t-bpy]), 7.41 (2 H, m, 5,5'-[Bu^t-bpy]), 7.22 (2 H, s, 5-C₄H₅N), 6.20 (2 H, m, 4-C₄H₅N), 6.00 (2 H, s, 3-C₄H₅N), 4.05 (2 H, d, ²J = 14.2 Hz, C₅H₄NCH₂N), 4.03 (1 H, s, C₄H₃NCH₂N), 3.47 (2 H, d, ²J = 13.8 Hz, C₅H₄NCH₂N), 3.45 (1 H, s, C₄H₃NCH₂N), 1.86 (3 H, s, C₄H₃NCH₂NCH₃), 1.40 (18 H, s, C(CH₃)₃). ¹³C{¹H} NMR (CDCl₃): δ = 166.6 (2,2'-[Bu^t-bpy]), 153.0 (4,4'-[Bu^t-bpy]), 150.5 (6,6'-[Bu^t-bpy]), 140.9 (4-C₅H₅N), 136.8 (2-C₄H₅N), 136.1 (3,3'-5,5'-[Bu^t-bpy]), 128.0

(5-C₄H₅N), 124.5 (3-C₅H₅N), 119.7 (2-C₅H₅N), 109.0 (4-C₄H₅N), 103.6 (3-C₄H₅N), 59.5 (C₅H₄NCH₂N), 45.7 (C₅H₄NCH₂NCH₃), 35.8 (C(CH₃)₃-[Bu^t-bpy]), 30.3 (C(CH₃)₃-[Bu^t-bpy]). Absorption spectrum: λ_{max} = 343 nm, ε = 12 700 cm⁻¹ M⁻¹. Elemental analysis for TiC₃₄H₄₂N₇-BF₄, found (calcd): C, 58.69 (59.74); H, 6.14 (6.21); N, 14.11 (14.35).

Procedure for the Kinetic Experiments. All manipulations were done in an MBraun inert atmosphere glovebox under an atmosphere of dry nitrogen. In a 1 mL volumetric flask was loaded catalyst (0.1 Ti-equiv, 0.04 mmol Ti), aniline (3 equiv, 1.2 mmol), FeCp₂ (0.2 M solution in toluene, 250 μL), and alkyne (1 equiv, 0.4 mmol). The solution was diluted to 1 mL with toluene and transferred to a J-Y NMR tube. The tube was removed from the drybox and heated in an oil bath at 100 °C, and the concentration of 1-phenylpropyne was monitored as a function of time by ¹H NMR spectroscopy. The observed pseudo-first-order rate constants using this procedure for Ti(NMe₂)₂(dpma) (**1**), Ti(NPh)(NHMe₂)₂(dpma) (**2**), and [Ti(NPh)(dpma)]₂ (**3**) were 3.9 × 10⁻⁶, 3.6 × 10⁻⁶, and 3.6 × 10⁻⁶ s⁻¹.

Attempted Hydroamination of 1-Hexyne with 1,1-Dimethylhydrazine Using 1, 6, and 7 as Catalyst. To a solution of H₂NNMe₂ (228 μL, 3 mmol) and 1-hexyne (115 μL, 1 mmol) in 30 mL of toluene was added Ti(NMe₂)₂(dpma) (**1**) (65 mg, 0.2 mmol), Ti(NHNMe₂)₂(dpma) (**6**) (70 mg, 0.2 mmol), or [Ti(NNMe₂)(dpma)]₂ (**7**) (29 mg, 0.05 mmol). The reaction mixtures were sealed in a 50 mL pressure tube and put in a 100 °C oil bath for 24 h. The vessels were returned to the drybox. The generation of hydroamination product was probed by GC/FID in comparison with authentic samples. The volatiles of the reaction mixtures were removed in vacuo, and the resulting residues were analyzed by ¹H NMR for investigation of the titanium complexes prepared. The reaction involving **1** had generated **7** as the major titanium product observed. No hydroamination product was observed when either **6** or **7** were used. Trace amounts of hydroamination product were observed with **1** as catalyst.

Acknowledgment. The authors gratefully acknowledge the financial support of the Petroleum Research Fund administered by the American Chemical Society, Center for Fundamental Materials Research at MSU, Department of Energy-Defense Programs, Office of Naval Research, and Michigan State University. A.L.O. thanks Mitch Smith, Seth N. Brown, Dan Nocera, Zhi-Heng Loh, and Jim McCusker for many interesting and helpful discussions. The authors also appreciate the aid of James T. Ciszewski with some of the X-ray diffraction studies.

Supporting Information Available: Supporting Information Available: Tables of crystallographic data including refinement parameters, coordinates, bond distances, and bond angles. Emission spectra for **10-I** and 1-aminopyridinium iodide. This material is available free of charge via the Internet at <http://pubs.acs.org>. See any current masthead page for ordering information and Web access instructions.

JA038320G